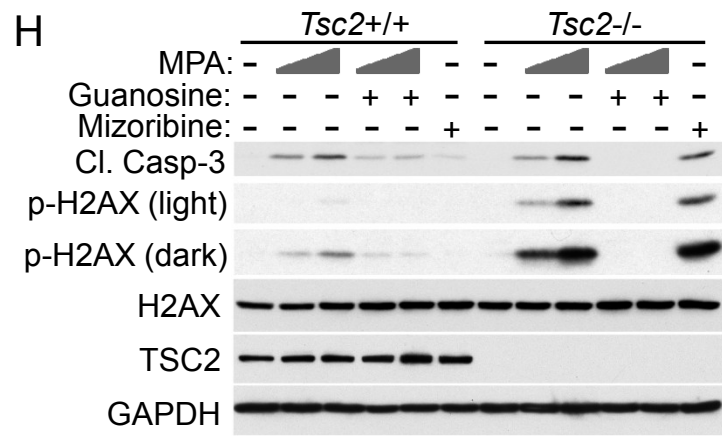
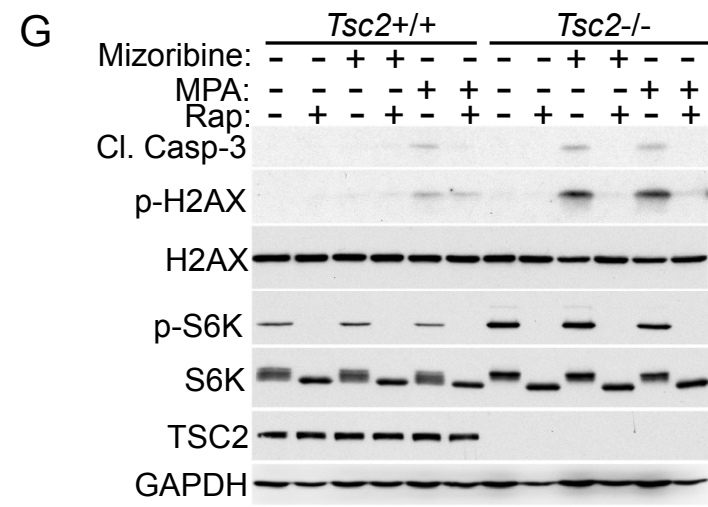
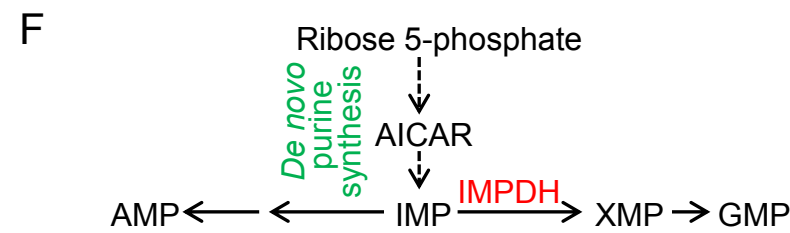
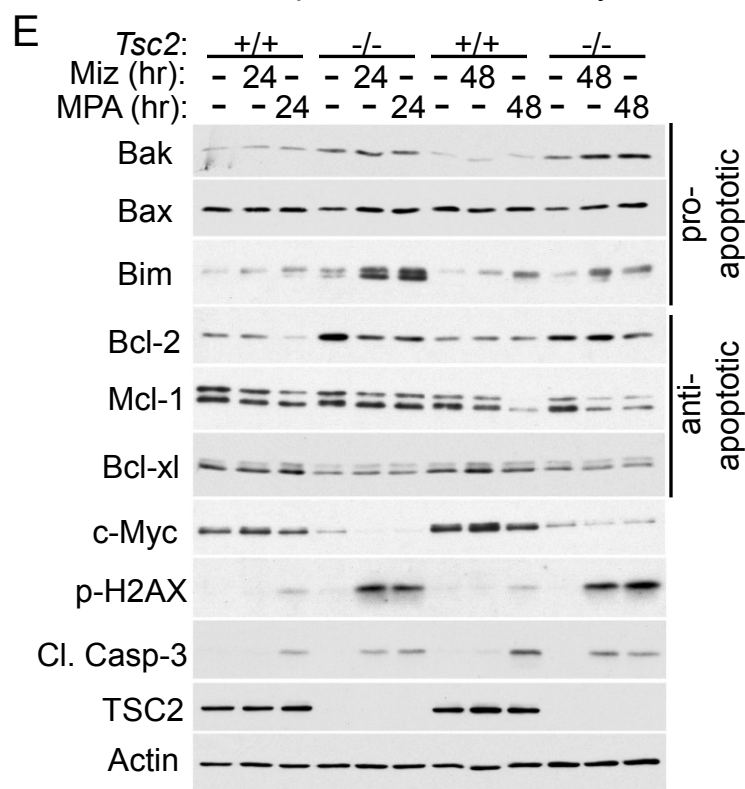
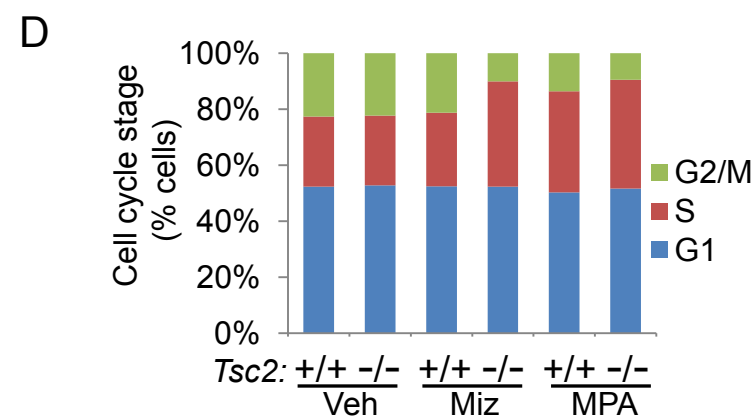
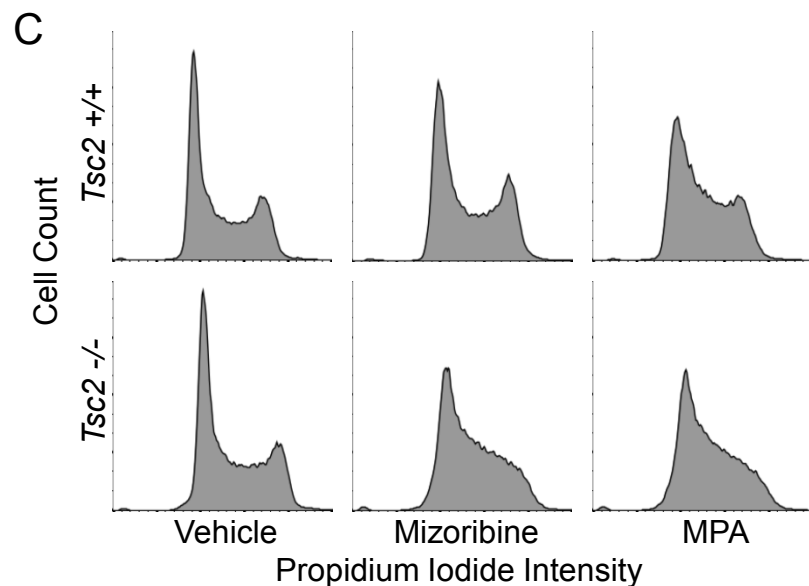
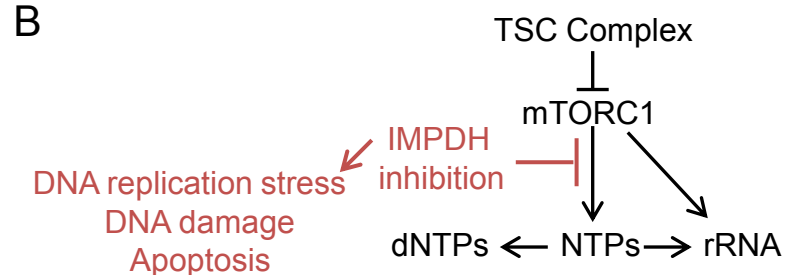
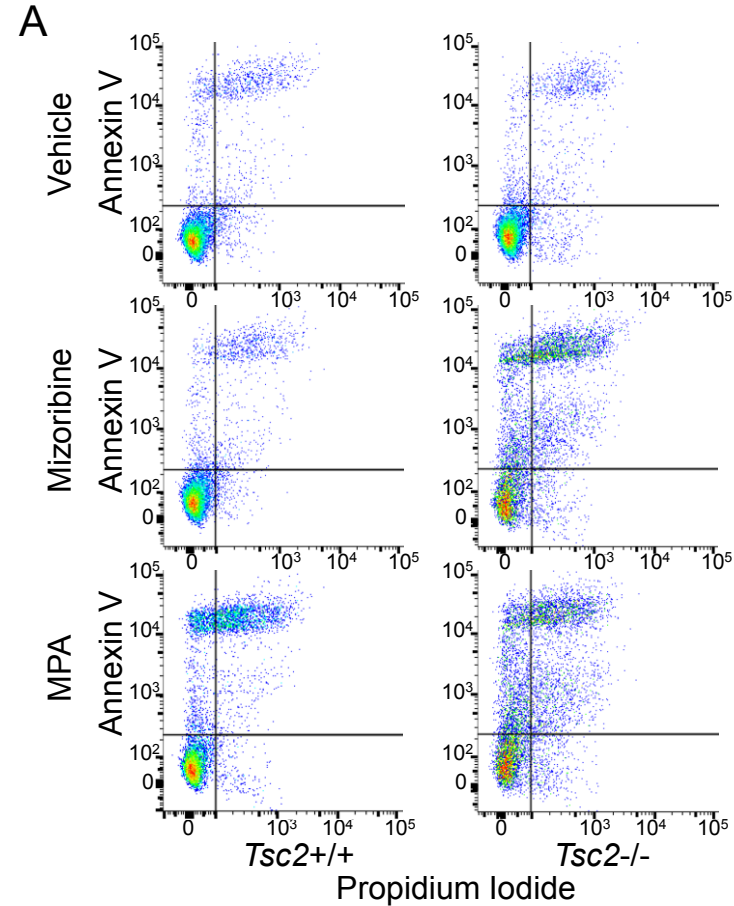


**Figure S1. Supplemental data supporting Figure 1**

(A-H) Viable cell counts in littermate derived *Tsc2*<sup>+/+</sup> and *Tsc2*<sup>-/-</sup> MEFs treated 72 hrs with vehicle or given concentrations of the indicated compounds, graphed as percent of vehicle treated cells. n = 3 independent experiments. (I,J) Viable cell counts in human *TSC2*<sup>-/-</sup> 621-101 cells stably reconstituted with empty vector or wild-type TSC2 (I) or HeLa cells with stable shRNA-mediated knockdown of TSC2 or luciferase control (J) treated for 48 hrs with indicated concentrations of mizoribine or MPA and graphed as percent of vehicle treated cells. n = 3 independent experiments.

Graphical data are represented as mean of indicated replicates, error bars represent  $\pm$  SEM. \*p < 0.05, #p < 0.01 by two-tailed Student's t test.



## Figure S2. Supplemental data supporting Figures 1 and 2

(A) Representative Annexin V/propidium iodide plots from the experiment in Figure 1D. (B) Model of the effects of IMPDH inhibitors as it relates to TSC-mTORC1 signaling. mTORC1 induces ribosomal RNA synthesis, greatly increasing cellular demand for nucleotides (NTPs), which is met by the parallel induction of *de novo* nucleotide synthesis. IMPDH inhibitors uncouple these processes, leading to a reduction in the NTP pool available for conversion to dNTPs required for DNA synthesis, thus causing unresolved DNA replication stress, DNA damage, and apoptosis selectively in TSC-deficient cells with high mTORC1 activity. (C) Cell-cycle distributions, measured by propidium iodide intensity, of *Tsc2*<sup>+/+</sup> and *Tsc2*<sup>-/-</sup> MEFs treated for 16 hr with 2  $\mu$ M mizoribine or 250 nM MPA. Data shown are representative of at least two independent experiments. (D) Quantification of data in (C), graphed as percent of the total population. n = 2 independent experiments. (E) Cells in (C) were treated for 24 or 48 hrs with 2  $\mu$ M mizoribine or 250 nM MPA followed by immunoblotting for indicated proteins. Results are representative of two independent experiments. (F) Schematic of the *de novo* purine synthesis pathway, highlighting the position of the intermediate AICAR upstream of IMPDH, the first enzyme in the guanylate synthesis branch. (G) Cells in (C) were treated for 48 hrs with 2  $\mu$ M mizoribine or 250 nM MPA alone or in combination with 20 nM rapamycin followed by immunoblotting for indicated proteins. Results are representative of at least two independent experiments. (H) Cells in (C) were treated for 48 hrs as indicated with MPA (200 or 300 nM), guanosine (50  $\mu$ M) or mizoribine (2  $\mu$ M) followed by immunoblotting for indicated proteins. Results are representative of at least two independent experiments.

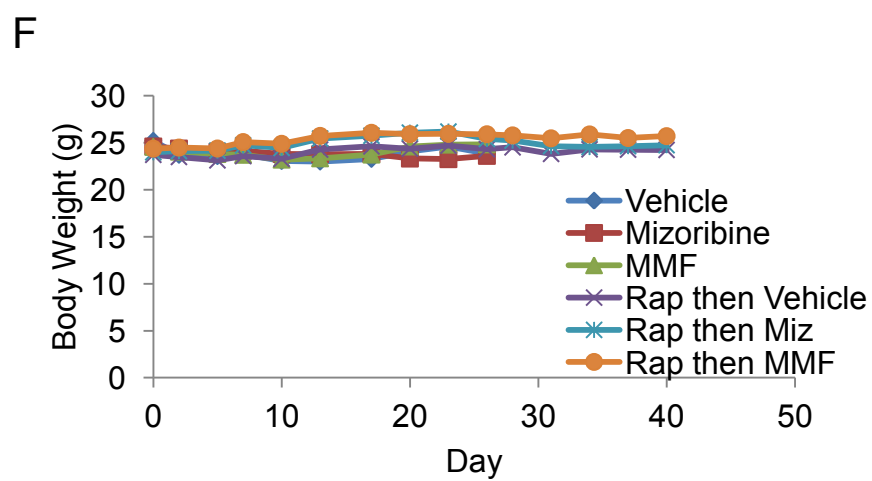
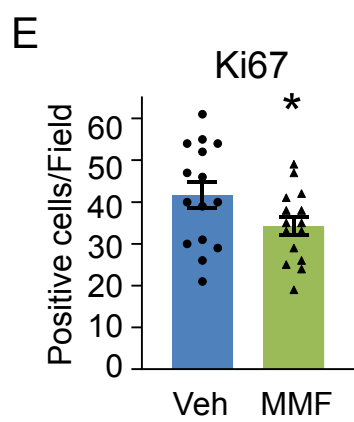
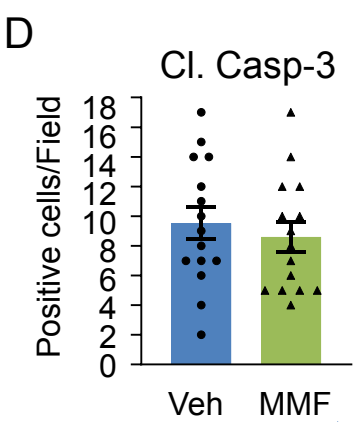
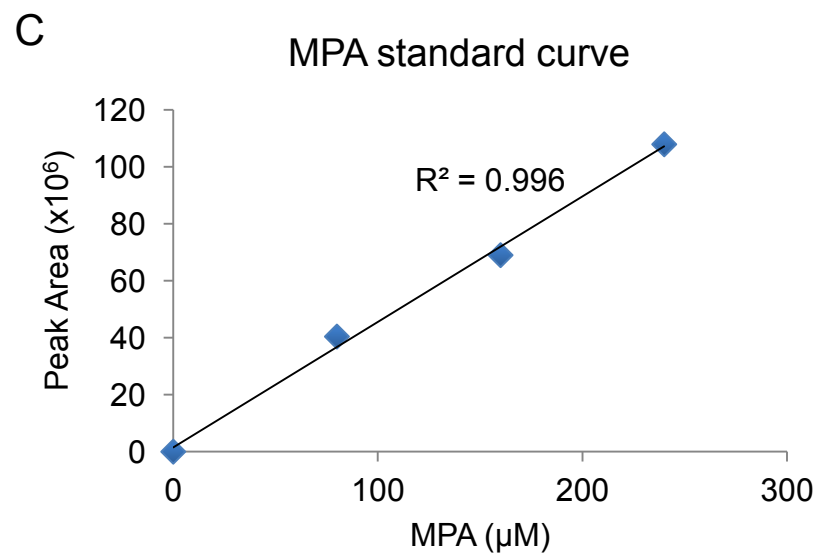
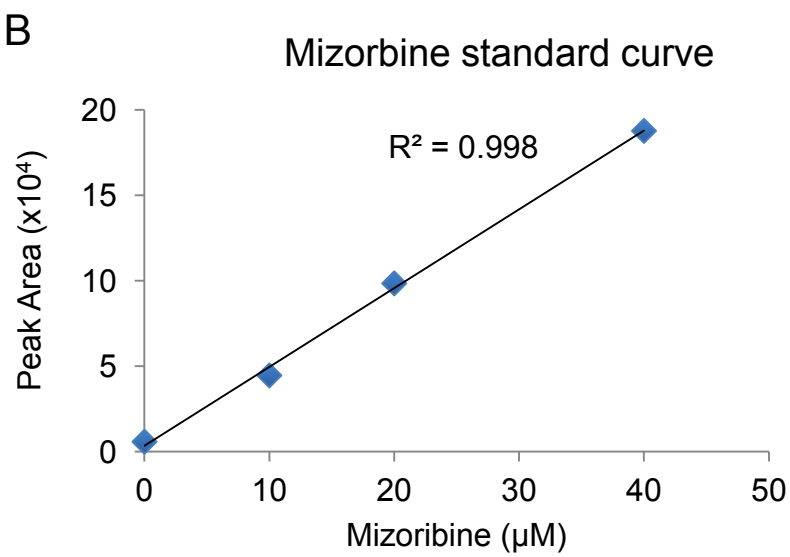
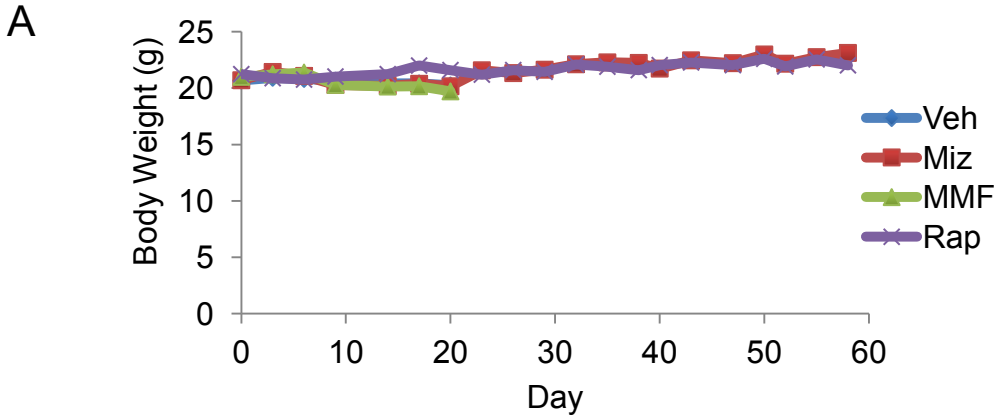


**Figure S3. Supplemental data supporting Figures 3 and 4**

(A) Total body weight of mice in Figure 3B. n = 6 mice per group. (B,C) Mizoribine and MPA standard curves used to quantify plasma concentrations in Figure 3C. Mizoribine or MPA were mixed into plasma from untreated mice at the indicated final concentrations. Metabolites were extracted from these standard samples alongside plasma from vehicle-, mizoribine- and MMF-treated mice, and mizoribine and MPA were measured by LC-MS/MS. (D,E) Quantification of (D) cleaved caspase-3 and (E) Ki67 staining in Figure 3D. Staining-positive cells per field of view were counted in 5 tumors per group in a blinded fashion, with 3 non-overlapping fields counted per tumor. (F) Total body weight of mice in Figure 4B. n = 3 mice per group

Graphical data are presented as mean of indicated replicates  $\pm$  SEM. \*p < 0.05 by two-tailed Student's t test.

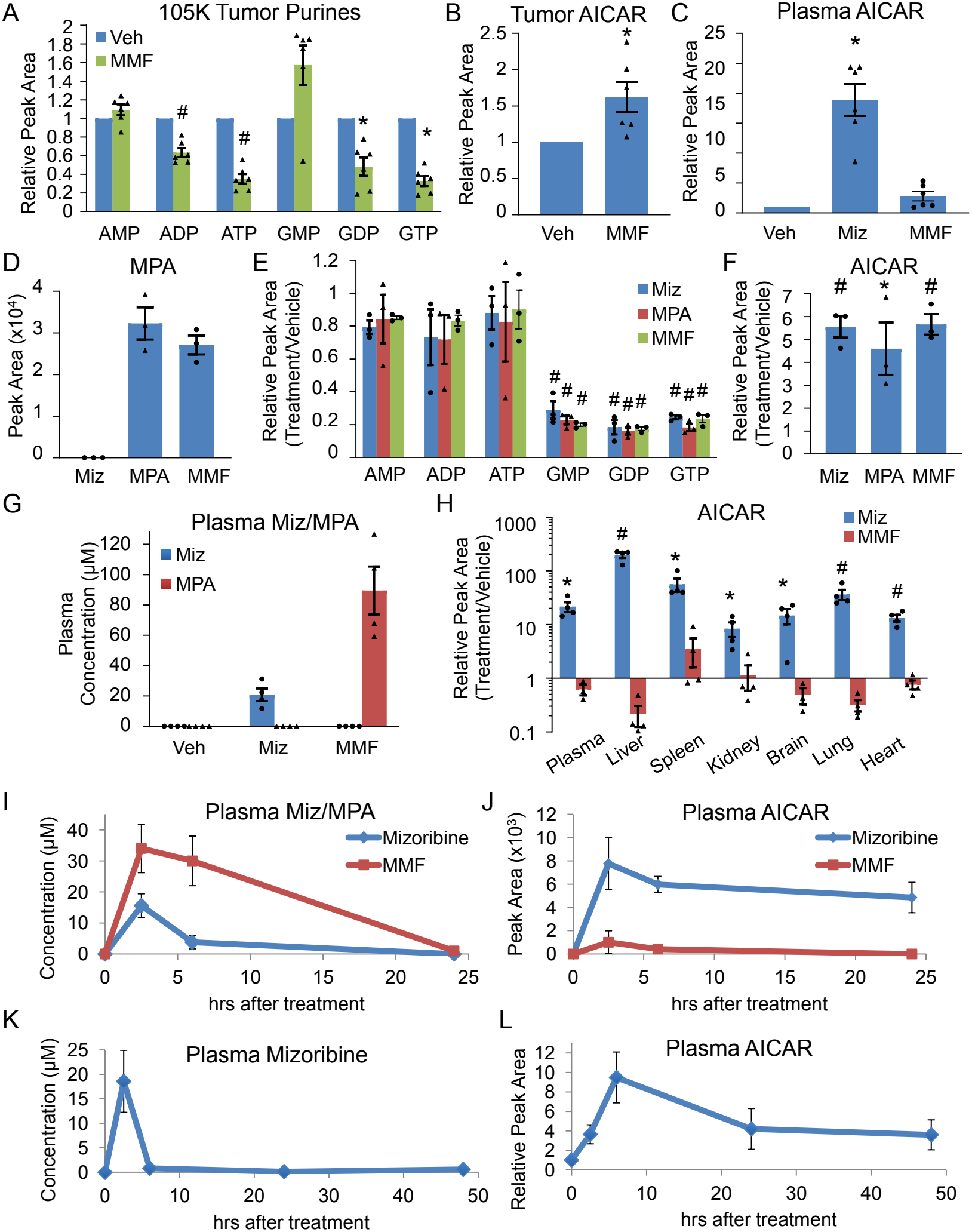


#### Figure S4. Supplemental data supporting Figure 5

(A-C) Steady state LC-MS/MS-based metabolite profiling of 105K xenograft tumors or plasma collected from the mice in Figure 3B treated with vehicle (n = 6) or MMF (n = 6). Peak area values relative to vehicle-treated mice of (A) tumor adenylates and guanylates, (B) tumor AICAR, or (C) plasma AICAR. (D-F) Indicated metabolites measured by LC-MS/MS in *Tsc2*<sup>+/+</sup> and *Tsc2*<sup>-/-</sup> MEFs treated for 16 hrs with vehicle, mizoribine (2  $\mu$ M), MPA (250 nM), or MMF (250 nM). The values in (E,F) are shown relative to vehicle-treated cells. n = 3 biological replicates from a single experiment. (G,H) C57BL/6J mice were treated daily by oral gavage with vehicle, mizoribine (45 mg/kg) or an equimolar dose of MMF (75 mg/kg) for 7 days. n = 4 mice/group. (G) Mizoribine and MPA concentrations in plasma collected 2.5 hrs after the final treatment. (H) AICAR levels measured by LC-MS/MS in the indicated tissues with peak area values graphed on a log<sub>10</sub> scale relative to AICAR levels in tissues from vehicle-treated mice. (I,J) NSG mice were given a single dose of mizoribine (50 mg/kg) or MMF (50 mg/kg) by oral gavage and plasma was collected at indicated time points for LC-MS/MS measurement of (I) mizoribine and MPA concentration and (J) AICAR levels. n = 3 mice for each treatment and time point. (K,L) C57BL/6J mice were given a single dose of mizoribine (100 mg/kg by i.p. injection) and plasma was collected at indicated time points for LC-MS/MS measurement of (K) mizoribine concentration and (L) AICAR levels. n = 3 mice for each time point.

Graphical data are represented as mean of indicated replicates, error bars represent  $\pm$  SEM. \*p < 0.05, #p < 0.01 by two-tailed Student's t test.



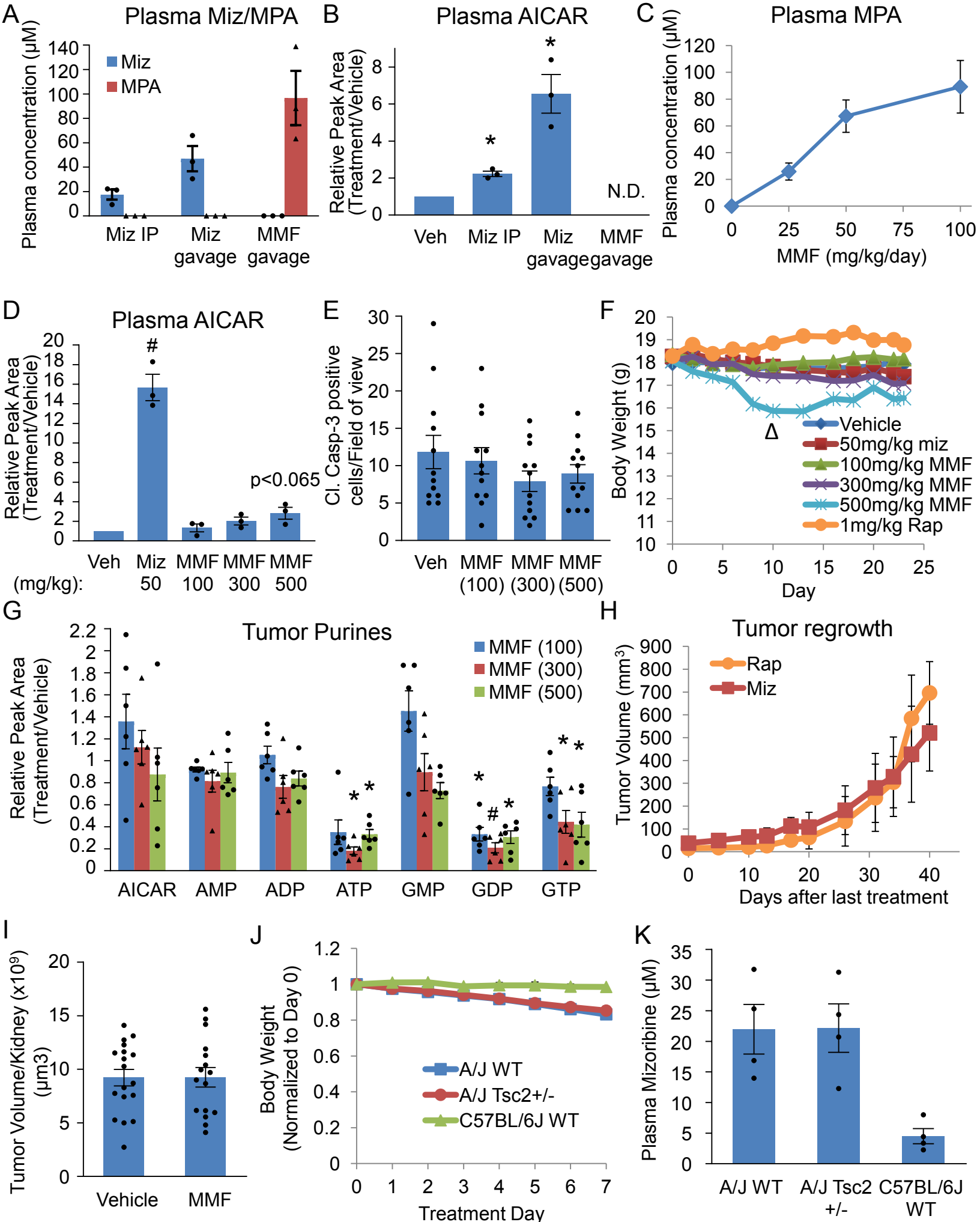


### Figure S5. Supplemental data supporting Figures 6 and 7

(A,B) C57BL/6J mice were treated daily for 3 days with mizoribine (100 mg/kg) by i.p. injection, mizoribine (100 mg/kg) by oral gavage, or an equimolar dose of MMF (167 mg/kg) by oral gavage. (A) Mizoribine and MPA concentration and (B) AICAR levels were measured by LC-MS/MS in plasma collected 2.5 hrs after the final treatment, with AICAR peak area values graphed relative to vehicle-treated mice. n = 3 mice per group. N.D. = not detected. (C) MPA concentration in plasma from C57BL/6J mice treated daily for 4 days with MMF by oral gavage with indicated doses. n = 3 mice per group. (D) AICAR levels in plasma from the mice in Figure 6A, measured by LC-MS/MS and graphed relative to vehicle-treated mice. (E) Quantification of cleaved caspase-3 staining from Figure 7A. Staining-positive cells per field were counted in 4 tumors per group in a blinded fashion, with 3 non-overlapping fields counted per tumor. (F) Total body weight of mice in Figure 6D. Beginning on day 10 (indicated by  $\Delta$ ), every 3<sup>rd</sup> day of treatment was skipped in the 500 mg/kg MMF group to mitigate weight loss. (G) Indicated metabolites measured by LC-MS/MS on extracts from 105K xenograft tumors collected from the MMF-treated mice in Figure 6D, resected 3 hrs after the final treatment, are shown relative to tumor metabolites from vehicle-treated mice. n = 6 tumors per group. (H) Volume of tumors measured every 3<sup>rd</sup> day during the regrowth phase in Figure 7D. (I) Kidney tumor-bearing *Tsc2*<sup>+/-</sup> mice on the A/J strain background were treated with vehicle or MMF (75 mg/kg/day) by oral gavage for 1 month beginning at 7 months of age, with tumor volume per kidney measured in serial H&E-stained sections. n = 8 mice per group. (J,K) Mice of the indicated genotypes and strain backgrounds were treated with mizoribine (30 mg/kg/day) for 7 days by oral gavage. n = 4 mice per group. (J) Total body weight measured daily. (K) Mizoribine concentration in plasma collected 2.5 hrs after the final treatment.

Graphical data are represented as mean of indicated replicates, error bars represent  $\pm$  SEM. \*p < 0.05 by two-tailed Student's t test.